



RESEARCH ARTICLE

WILEY

A novel geometry-based analysis of hippocampal morphometry in mesial temporal lobe epilepsy

Laura Fischbach¹ | Tobias Bauer¹  | Kersten Diers² | Juri-Alexander Witt¹ | Mar Bruges³ | Valeri Borger⁴ | Martin Schidlowski¹ | Attila Rácz¹ | Tobias Baumgartner¹ | Randi von Wrede¹ | Daniel Paech⁵ | Bernd Weber⁶ | Alexander Radbruch⁵ | Hartmut Vatter⁴ | Albert J. Becker³ | Hans-Jürgen Huppertz⁷ | Christoph Helmstaedter¹ | Rainer Surges¹ | Martin Reuter^{2,8,9} | Theodor Rüber¹ 

¹Department of Epileptology, University Hospital Bonn, Bonn, Germany

²AI in Medical Imaging, German Center for Neurodegenerative Diseases (DZNE), Bonn, Germany

³Department of Neuropathology, University Hospital Bonn, Bonn, Germany

⁴Department of Neurosurgery, University Hospital Bonn, Bonn, Germany

⁵Department of Neuroradiology, University Hospital Bonn, Bonn, Germany

⁶Institute of Experimental Epileptology and Cognition Research, University Hospital Bonn, Bonn, Germany

⁷Swiss Epilepsy Clinic, Klinik Lengg AG, Zurich, Switzerland

⁸Athinoula A. Martinos Center for Biomedical Imaging, Massachusetts General Hospital, Boston, Massachusetts, USA

⁹Department of Radiology, Harvard Medical School, Boston, Massachusetts, USA

Correspondence

Theodor Rüber, Department of Epileptology, University Hospital Bonn, Venusberg-Campus 1, Bonn 53127, Germany.

Email: theodor.rueber@ukbonn.de

Funding information

University of Bonn, Grant/Award Numbers: 2020-4-06, 2019-4-07

Abstract

Hippocampal volumetry is an essential tool in researching and diagnosing mesial temporal lobe epilepsy (mTLE). However, it has a limited ability to detect subtle alterations in hippocampal morphometry. Here, we establish and apply a novel geometry-based tool that enables point-wise morphometric analysis based on an intrinsic coordinate system of the hippocampus. We hypothesized that this point-wise analysis uncovers structural alterations not measurable by volumetry, but associated with histological underpinnings and the neuropsychological profile of mTLE. We conducted a retrospective study in 204 individuals with mTLE and 57 age- and gender-matched healthy subjects. FreeSurfer-based segmentations of hippocampal subfields in 3T-MRI were subjected to a geometry-based analysis that resulted in a coordinate system of the hippocampal mid-surface and allowed for point-wise measurements of hippocampal thickness and other features. Using point-wise analysis, we found significantly lower thickness and higher FLAIR signal intensity in the entire affected hippocampus of individuals with hippocampal sclerosis (HS-mTLE). In the contralateral

Laura Fischbach and Tobias Bauer contributed equally to this study.

This is an open access article under the terms of the [Creative Commons Attribution-NonCommercial](https://creativecommons.org/licenses/by-nc/4.0/) License, which permits use, distribution and reproduction in any medium, provided the original work is properly cited and is not used for commercial purposes.

© 2023 The Authors. *Human Brain Mapping* published by Wiley Periodicals LLC.

hippocampus of HS-mTLE and the affected hippocampus of MRI-negative mTLE, we observed significantly lower thickness in the presubiculum. Impaired verbal memory was associated with lower thickness in the left presubiculum. In HS-mTLE histological subtype 3, we observed higher curvature than in subtypes 1 and 2 (all $p < .05$). These findings could not be observed using conventional volumetry (Bonferroni-corrected $p < .05$). We show that point-wise measures of hippocampal morphometry can uncover structural alterations not measurable by volumetry while also reflecting histological underpinnings and verbal memory. This substantiates the prospect of their clinical application.

KEYWORDS

differential geometry, epilepsy, hippocampal sclerosis, magnetic resonance imaging, shape analysis

1 | INTRODUCTION

Mesial temporal lobe epilepsy (mTLE) is the most common form of focal epilepsy in adults undergoing presurgical assessment in specialized epilepsy centers. It is described by clinical, electrophysiological, histopathological, and radiological features (Engel Jr., 1996; Semah et al., 1998; Téllez-Zenteno & Hernández-Ronquillo, 2012). The hippocampus is the pathological substrate of mTLE and its unilateral neurosurgical resection is a principal treatment option (Blümcke et al., 1999; Schwartzkroin, 1986; Wieser, 1988). In a large case series of 1109 of operated mTLE cases from two major epilepsy centers in Europe (Department of Epileptology at the University Hospital Bonn and Institute of Neurology at the University College of London), Blümcke et al. (2002) found hippocampal sclerosis (HS) in approximately 65%. In the general population of people with mTLE, however, the prevalence of HS is much lower, since people with HS are more likely to undergo epilepsy surgery (Engel Jr., 1996). HS is defined by neuronal cell loss and reactive astrogliosis (Blümcke et al., 2012; Thom, 2014). Four histological subtypes of HS are differentiated based on specific patterns of neuronal cell loss in the pyramidal cell layer of the different cornu ammonis (CA) regions (Blümcke et al., 2013, see Table 1). Previous studies have demonstrated that these subtypes have different prognoses in terms of memory performance and postoperative seizure control (Blümcke et al., 2007; Coras & Blümcke, 2015; Saghati et al., 2018; Stefan et al., 2009). Hence, it would be of great clinical benefit if histological classification, which by its nature can only be performed postoperatively, could serve as a foundation for clinical decision-making preoperatively.

Conventional neuroradiological reading of 3T magnetic resonance imaging (MRI), however, yields no structural abnormalities in up to one-third of all individuals with mTLE (MRI-negative; Muhlhofer et al., 2017). In MRI-negative mTLE cases, the proportion of satisfying postoperative seizure outcomes has been shown to be lower than in cases with hippocampal lesions confirmed preoperatively on MRI (Immonen et al., 2010; Yin et al., 2013). Previous research suggests that structural alterations of the presubiculum are of subordinate

importance in epileptogenesis, but rather a consequence of recurring epileptic seizures (Maccotta et al., 2015). This leads to the hypothesis that alterations explicitly in the presubiculum should also be expected in MRI-negative mTLE. While ultra high-field MRI (7T) increases the diagnostic yield for individuals with mTLE, 3T will remain the available standard for the foreseeable future even in epilepsy centers (Opheim et al., 2021; Santyr et al., 2017; Wang et al., 2020). Hence, it is hoped that an analysis of hippocampal morphometry based on universally available 3T MR-images will allow for a preoperative estimation of the histological subtype and decrease the number of MRI-negative mTLE cases.

Hippocampal volume is considered an established imaging marker for structural alterations in neurological and psychiatric disorders, however, it has very limited ability to detect subtle microstructural abnormalities of distinct hippocampal subfields (Wachinger et al., 2016). A novel analysis of hippocampal morphometry would have to outperform existing approaches in three respects: First, it should be based on the internal architecture of the hippocampus. Second, hippocampal subfields should not be the only reference for anatomical localization, as subfield delineation is subject to uncertainty

TABLE 1 ILAE classification of hippocampal sclerosis.

	HS type 1	HS type 2	HS type 3	No HS
CA1	2	1–2	0	0
CA2	0–2	0–1	0–1	0
CA3	0–2	0–1	0–1	0
CA4	2	0–1	1–2	0

Note: Scoring system of neuronal cell loss and gliosis defined for CA1–4 as follows: 0 = no neuronal cell loss or moderate astrogliosis only; 1 = moderate neuronal cell loss and gliosis; 2 = severe neuronal cell loss and fibrillary astrogliosis (Blümcke et al., 2013).

Abbreviations: CA, cornu ammonis; HS, Hippocampal sclerosis.

and may be driven by atlas information rather than image contrast. Third, complementary metrics such as hippocampal thickness or curvature should be provided, as morphometric changes of the hippocampus are manifold and cannot be captured by volumetric changes alone. To address these issues, in the present work, we establish a novel geometry-based algorithm (Diers et al., 2023) that creates a geometric representation of the internal structure of the hippocampus and uses hippocampal unfolding to provide an intrinsic anatomical coordinate system for the point-wise analysis of morphometric alterations. We hypothesize that this point-wise analysis will uncover structural alterations that are not detectable with volumetry and that can be linked to the histological underpinnings and neuropsychological profile of mTLE. We test these hypotheses in three steps: (1) Investigating MRI-negative mTLE for previously undetected morphometric correlates, especially in the presubiculum, using the new point-wise analysis, (2) relating preoperative morphometric measurements to postoperative histological classification in HS, (3) showing an association between the novel geometry-based imaging marker and neuropsychological outcome. It is the aim of this study to establish a novel imaging biomarker to fully exploit routine 3T MRI in the presurgical evaluation of mTLE.

2 | MATERIALS AND METHODS

2.1 | Study group

This retrospective study incorporates three study groups: First, we ascertained all individuals who underwent presurgical evaluation and neurosurgical resection of one hippocampus with postoperatively confirmed HS between 2007 and 2018 ($n = 146$). To be included in this study, all individuals with unilateral HS and mTLE (HS-mTLE, total $n = 146$) had to be histologically classified and further differentiated into the subtypes one (HS1, 129/146), two (HS2, 14/149), and three (HS3, 3/149) according to ILAE criteria (Blümcke et al., 2013). We refer to the surgically resected hippocampus as *affected* hippocampus, and to the non-resected hippocampus as *contralateral* hippocampus. Second, we ascertained all individuals who underwent preoperative

evaluation at the Department of Epileptology at the University Hospital Bonn between 2007 and 2018 with clinically diagnosed mTLE and normal MRI (MRI-negative mTLE; $n = 58$). Inclusion criteria for this group were as follows: (1) Interictal epileptiform discharges in the temporal lobe and electroclinical presentation of at least three stereotypical mesiotemporal seizures in video EEG monitoring, (2) Normal 3T MRI assessed by neuroradiology specialists. In addition, most subjects either underwent additional imaging diagnostic by ^{18}F -fludeoxyglucose positron emission tomography (^{18}F FDG-PET, 30/58) or ictal and interictal single photon emission computed tomography (SPECT, 14/58) to confirm a temporal focus. In 21/58, mTLE was confirmed in invasive EEG recordings. Of all those individuals, 11/58 were bilaterally affected according to EEG recordings, seizure semiology, and neuropsychological testing. In this case, both hippocampi were regarded as *affected* hippocampi, so a total of 69 *affected* and 47 *contralateral* hippocampi were examined in this group. Nine individuals were treated surgically, all of whom showed gliosis in the hippocampus according to neuropathological examination. Epilepsy surgery was not performed in the remaining 49 individuals. Third, we included 57 age- and gender-matched healthy subjects with no history of neurological disorders. Both hippocampi of the healthy subjects were used for analyses, so a total of 114 healthy hippocampi were included. Furthermore, we required at least one (presurgical) isotropic T1-weighted MRI to be available for all ascertained individuals. Based on requirements of the internal review board, only images acquired above 18 years of age were included. See Table 2 for an overview of the study cohort. The study was approved by the internal review board of the University Hospital Bonn. All participants provided written informed consent.

2.2 | Neuropsychological testing

In 120/146 individuals with HS-mTLE results of neuropsychological testing were available. Verbal learning and the overall memory performance were assessed using the verbal learning and memory test (Helmstaedter & Durwen, 1990). Abilities in figural memory were tested using the revised *Diagnosticum fuer Cerebralschaedigung*

TABLE 2 Demographic and clinical data for the mTLE subgroups and the healthy subjects.

	Number of subjects	Age at MRI (years)	Female	Affected side left	Impaired verbal memory
HS type 1	129	38.2 ± 14.4	69 (52%)	77 (58%)	70/108 (65%)
HS type 2	14	38.4 ± 14.1	5 (36%)	7 (50%)	7/12 (58%)
HS type 3	3	32.0 ± 9.5	1 (33%)	1 (33%)	—
all HS (type 1+2+3)	146	38.1 ± 14.2	74 (51%)	83 (57%)	77/120 (64%)
MRI-negative	58	36.5 ± 10.8	35 (60%)	30 (52%)	—
mTLE (HS+MRI-negative)	204	38.0 ± 13.5	109 (53%)	113 (55%)	—
Healthy subjects	57	36.4 ± 10.6	34 (60%)	—	—

Note: Mean ± standard deviation is presented. MRI-negative: Individuals with temporal lobe epilepsy and no correlates in magnetic resonance imaging. Abbreviations: HS, hippocampal sclerosis; mTLE, mesial temporal lobe epilepsy.

(Helmstaedter et al., 1991). Memory performance was regarded as impaired if the individual performance was at least one standard deviation below the mean of a normative sample.

2.3 | Image acquisition

All subjects, including the healthy subjects, received T1-weighted structural imaging on a 3T MRI at the University Hospital Bonn, either at the Department of Neuroradiology (91/146 HS-mTLE, 0/58 MRI-negative mTLE, 0/57 healthy subjects; Achieva, Philips, Best, The Netherlands) or at the Life & Brain Center (55/146 HS-mTLE, 58/58 MRI-negative mTLE, 57/57 healthy subjects; Magnetom Trio, Siemens Healthineers, Erlangen, Germany). From all sites, 3D T1-weighted images with a high resolution of either 1.0 or 0.8 mm isotropic voxel size were included in the study. In cases where more than one 3D T1-weighted scan was available, we included the latest scan before surgery. Furthermore, a 3D FLAIR scan with 1.0 mm isotropic voxel size was available for 80/146 individuals with HS-mTLE, 57/58 individuals with MRI-negative mTLE and 25/57 healthy subjects. All 3D FLAIR scans were performed at the Life & Brain Center.

2.4 | Image preprocessing and segmentation

Segmentation of cortical and subcortical structures of T1-weighted images using FreeSurfer (v7.0, <https://surfer.nmr.mgh.harvard.edu/>; Dale et al., 1999) was followed by automated segmentation of the hippocampal subfields and nuclei of the amygdala (Iglesias et al., 2015; Saygin et al., 2017). Visual inspection for accuracy and alignment of the results was performed at every step of segmentation, focusing on the hippocampus. Images with either failed hippocampal segmentation, inaccurate tetrahedral mesh models or sheet-like representations were excluded from the analysis (32/236, −14%). FLAIR images were preprocessed using FSL. A brain extraction with subsequent bias field correction was performed using FSL. Intensity normalization was performed as described in detail by Focke et al. (2008, 2009), Huppertz et al. (2011) and Wagner et al. (2013). In brief, white and gray matter masks were calculated for each subject using FSL, and average gray and white matter FLAIR signal intensities were extracted. An individual scaling factor was calculated by rescaling the average signal intensity of the FLAIR image (mean of white and gray matter signal intensity) to an arbitrary value of 100. This scaling factor was then applied to the entire FLAIR volume. FreeSurfer's within-subject, cross-modal registration was used to register the preprocessed FLAIR images to the T1-weighted images in the FreeSurfer space.

2.5 | Volumetric analysis

Volumetric analysis was conducted for the subfields segmented by the FreeSurfer toolbox, including the parasubiculum, presubiculum, subiculum, CA1, CA3, CA4, granule cell, and molecular layer of the

dentate gyrus (GC-ML-DG), the molecular layer, the hippocampus-amygdala-transition-area (HATA), fimbria, hippocampal tail, hippocampal body, hippocampal head and hippocampal fissure.

2.6 | Point-wise morphometric analysis

Hippocampal thickness analysis was performed by a novel, geometry-based algorithm which creates a parametric shape representation of the hippocampus (Diers et al., 2023). First, a 3D tetrahedral mesh model of the hippocampus was created from FreeSurfer's subfield segmentation. By cutting the mesh at the transitions of the hippocampal body to the head and tail, we obtained its anterior/posterior boundaries. Two other pairs of boundaries (interior/exterior and medial/lateral) were determined using the first eigenfunction of the anisotropic (i.e., curvature-aware) Laplace-Beltrami operator, which has been designed to have a value of zero at specific high mean curvature regions, such as the lateral and medial edges of the hippocampal body. Solving Poisson's equation for each pair of boundaries gives smooth parametric functions along the anterior–posterior, inner–outer, and medial–lateral dimensions of the hippocampal body. The level sets (“contours”) of these functions constitute a three-dimensional grid, from which we extracted inner, outer, and medial surfaces as sheet-like representations of the hippocampal body as well as an intrinsic 3D coordinate system of the hippocampal body. Correspondence of the coordinate system across subjects is achieved due to the anatomically consistent placement of the boundaries and parametric functions. Estimates of local hippocampal thickness were obtained by tracing streamlines along the interior/exterior dimension at fixed anterior/posterior and medial/lateral grid points (Figure 1). Similarly, the streamlines allow for a projection of signals from other modalities (e.g., co-registered FLAIR images) onto the medial surface. Finally, we computed the mean curvature of the medial surface as an additional characteristic of hippocampal geometry complementary to hippocampal thickness. While volumetric measures describe 19 regions throughout the entire hippocampus, it should be noted that the point-wise analysis covers only the presubiculum, subiculum, CA1, and CA2/3 subfields. The parasubiculum, granule cell and molecular layer of the dentate gyrus (GC-ML-DG), hippocampal molecular layer, hippocampus-amygdala-transition-area (HATA), fimbria, and hippocampal tail are not covered by the point-wise analysis.

2.7 | Statistical analysis

Statistical analysis was conducted in Python using the freely available toolboxes scipy (v1.5.0, <https://scipy.org>; Virtanen et al., 2020) and statsmodels (v0.11.1, <https://www.statsmodels.org/>; Seabold & Perktold, 2010), as well as Pymer4 (v0.7.8dev0, <https://eshinjolly.com/pymer4>; Jolly, 2018). Statistical comparisons were conducted in two or three steps: First, we tested for differences between groups using subfield-level volumetric measures as dependent variable; second, we conducted point-wise analysis on the hippocampal mid-

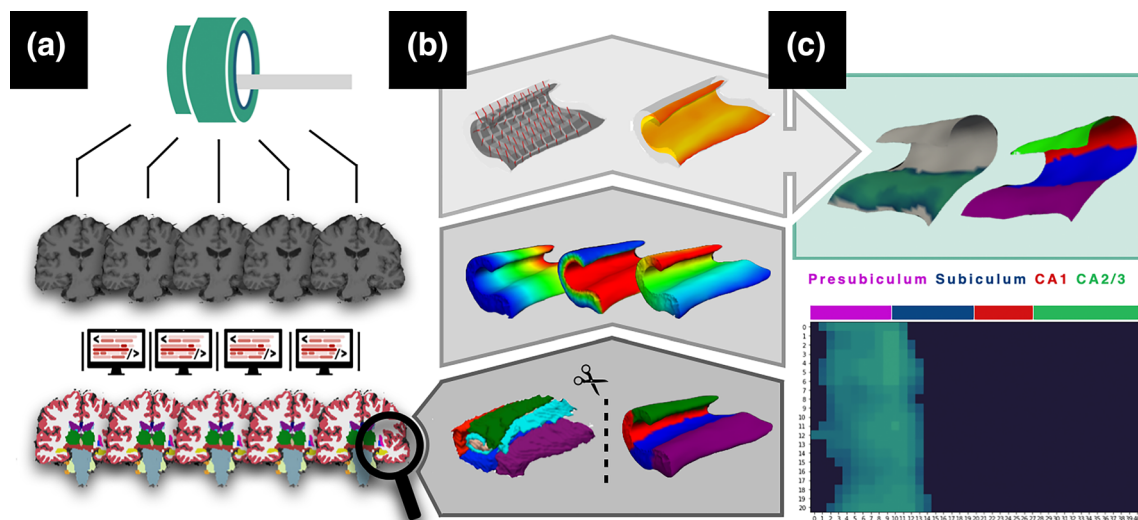


FIGURE 1 Illustration of the preprocessing, the novel geometry-based algorithm and mapping of results. (a) Top: Acquisition of T1-weighted 3T MR-images. Bottom: Segmentation of cortical and subcortical structures using FreeSurfer. (b) Bottom: A 3D tetrahedral mesh model of the hippocampus is created from FreeSurfer's subfield segmentation and cut at the junctions of the hippocampal body to the head and tail. Middle: Poisson equation for each pair of boundaries provides parametric functions along the anterior-posterior, inner-outer, and medial-lateral dimensions of the hippocampal body. Top: An internal grid of the hippocampus is created and estimates of hippocampal thickness are obtained by tracking the inner/outer dimension of the grid. (c) Top: Example three-dimensional plot of results and subfield boundaries on a healthy control hippocampus. Bottom: Mapping of the results to a two-dimensional coordinate system with only significant points being shown (green cluster).

surface using point-wise measures for thickness and FLAIR signal intensity as dependent variables. Third, if the point-wise analysis for the entire hippocampus did not yield significant results, but a hypothesis regarding a distinct subfield was to be tested, the point-wise analysis was repeated, limited to the respective subfield. To test for the group effects, we performed one-way analyses of variance (ANOVA), including age at MRI, sex, and affected side as covariates. As previous work suggests that the hippocampal subfield segmentation in FreeSurfer may be biased by different MRI setups (Brown et al., 2020; Quattrini et al., 2020), we have also included MRI sequence as a covariate in our model and confirmed our results in a subgroup analysis with all data acquired on the same scanner. In cases where both hippocampi of a subject were used in the analysis, a linear mixed-effects model incorporating an additional subject-level random intercept was applied instead. To address multiple comparisons in subfield-level volumetric analyses, a Bonferroni-correction to control for the family-wise error rate (FWER) was applied. In point-wise analysis, Threshold Free Cluster Enhancement (TFCE) was performed using the MNE Toolbox (v0.24.0, <https://mne.tools/stable/index.html>; Gramfort et al., 2014). We considered a p -value of $p < .05$ as statistically significant.

3 | RESULTS

3.1 | HS-mTLE versus healthy subjects

An ANOVA with the whole affected hippocampus as dependent variable showed a significant volume loss in individuals with HS-mTLE compared to healthy subjects (−30%, post-hoc t -test FWER-corrected

$p < .001$). ANOVAs with hippocampal subfields of the affected hippocampus as dependent variables revealed volume loss in individuals with HS-mTLE in the following subfields: parasubiculum (−13%), presubiculum (−25%), subiculum (−26%), CA1 (−33%), CA2/3 (−33%), CA4 (−36%), GC-ML-DG (−35%), molecular layer (−32%), HATA (−15%), fimbria (−25%), and hippocampal tail (−28%); post-hoc t -test, all FWER-corrected $p < .001$. See Online Table 1 for statistical details. In the contralateral hemisphere, we found significant volume loss of the fimbria (−13%; $p < .001$), but not in the subfields covered by point-wise analysis. See Online Table 2 for statistical details.

Point-wise morphometric analysis of hippocampal thickness between the affected hippocampus of the HS-mTLE group and healthy subjects revealed significantly lower thickness (FWER-corrected $p < .05$) in the presubiculum, subiculum, CA1, and the medial regions of CA2/3. Moreover, individuals with HS-mTLE showed higher FLAIR signal intensity in the subiculum, CA1, and CA2/3 in the affected hippocampus, however not in the presubiculum. Regarding the contralateral hemisphere, a point-wise analysis revealed lower hippocampal thickness in the presubiculum and no alterations of FLAIR signal intensity (Figure 2).

Volumetric and hippocampal thickness results were confirmed in a subgroup with data acquired on one same scanner only, see Online Tables 3 and 4 for volumetric analyses, and Online Figure 1 for hippocampal thickness analyses.

3.2 | MRI-negative mTLE versus healthy subjects

ANOVAs with the hippocampal volume and the hippocampal subfields both in the affected and contralateral side as dependent variables

HS-mTLE versus healthy subjects: Thickness and FLAIR analysis

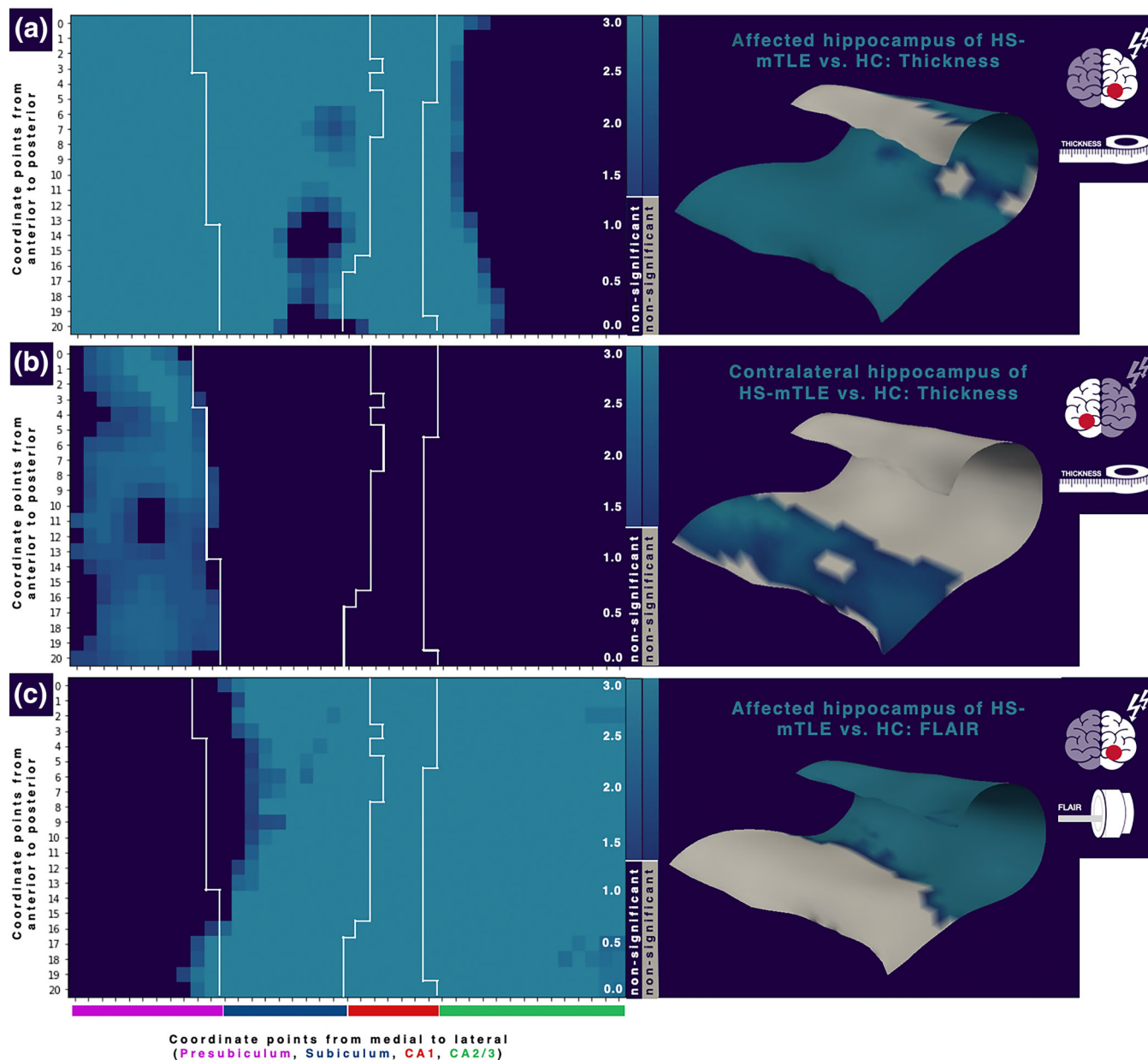


FIGURE 2 Individuals with HS-mTLE versus healthy subjects: Thickness and FLAIR analysis. (a) Thickness analysis of the affected hippocampus of individuals with HS-mTLE versus healthy subjects. (b) Thickness analysis of the contralateral hippocampus of HS-mTLE versus healthy subjects. (c) FLAIR analysis of the affected hippocampus of HS-mTLE versus healthy subjects. Left: Negative logarithms of significant p -values mapped along the intrinsic coordinate system of the hippocampus. Non-significant points are shown in dark-blue color. White lines: plotted boundaries of subfields, colored bars correspond to subfields. Right: Mapping of the negative logarithms of significant p -values onto the medial surface of a control hippocampus. CA, cornu ammonis; HC, healthy subjects; HS-mTLE, hippocampal sclerosis in individuals with mesial temporal lobe epilepsy.

revealed no significant differences between individuals with MRI-negative mTLE and healthy subjects, see Online Tables 5 and 6 for statistical details.

In point-wise analysis of hippocampal thickness, no significant clusters could be observed after FWER correction in the affected hippocampus. To test the hypothesis of alterations in the presubiculum, as in the contralateral hippocampus in individuals with HS-mTLE, we

repeated the point-wise analysis confined to mid-surface points assigned to the presubiculum. In this analysis, we observed a cluster with significantly lower thickness (FWER-corrected $p < .05$) located in the medial presubiculum. In the contralateral hemisphere, we found no significant alterations in point-wise analysis of hippocampal thickness across the entire hippocampus. A point-wise analysis confined to the contralateral presubiculum yielded a significant cluster (FWER-

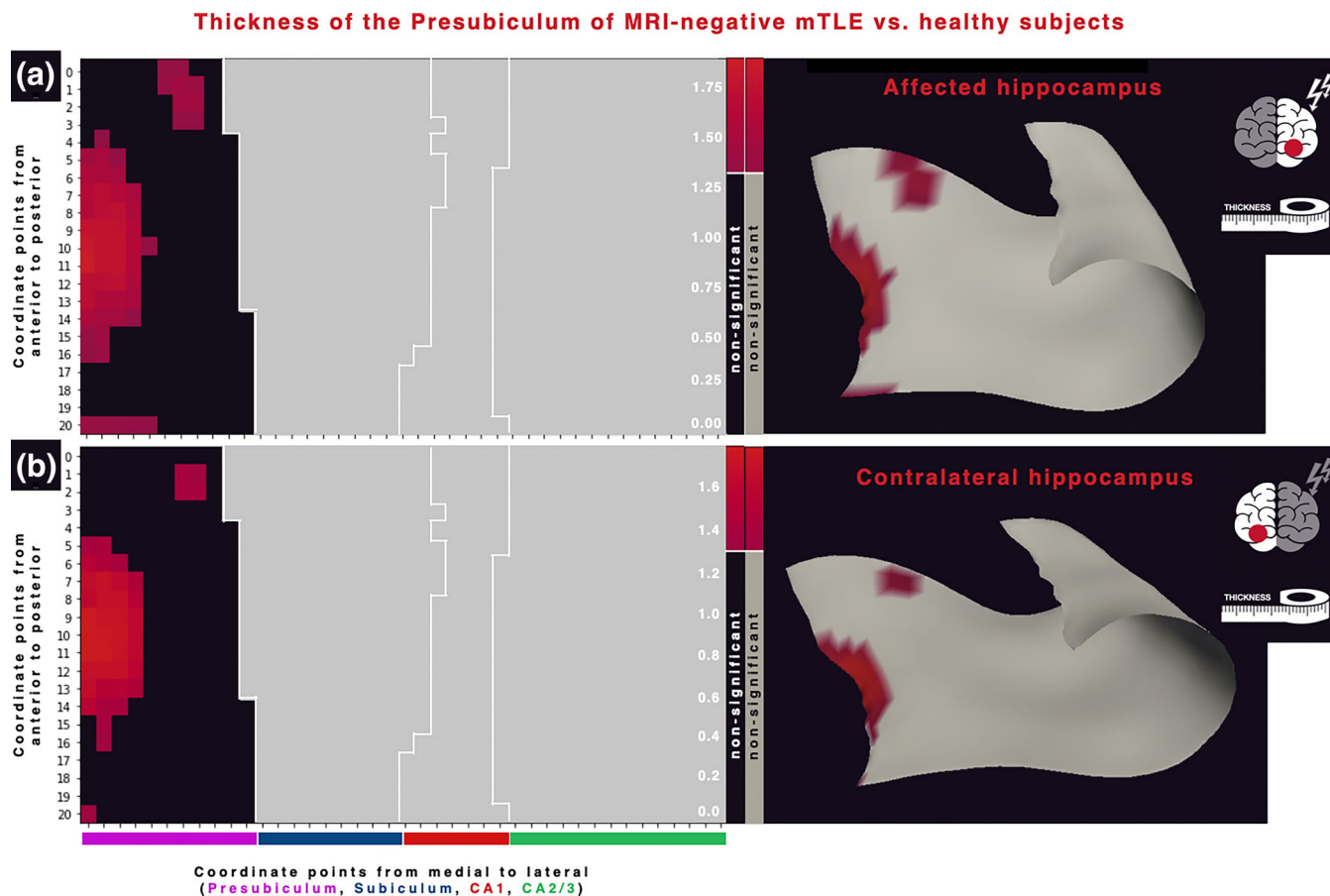


FIGURE 3 Individuals with MRI-negative mTLE versus healthy subjects: Thickness analysis. (a) Thickness analysis of the affected hippocampus of MRI-negative mTLE versus healthy subjects. (b) Thickness analysis of the contralateral hippocampus of MRI-negative mTLE versus healthy subjects. Left: Negative logarithms of significant p -values mapped along the intrinsic coordinate system of the presubiculum. Non-significant points are shown in black color. White lines: plotted boundaries of subfields, colored bars correspond to subfields. Right: Mapping of the negative logarithms of significant p -values onto the medial surface of a control hippocampus. CA, cornu ammonis; MRI-negative mTLE, individuals with mesial temporal lobe epilepsy and no correlates in magnetic resonance imaging.

corrected $p < .05$) in this subfield, similar to the affected hippocampus (Figure 3). Regarding FLAIR signal intensity, we found no clusters with altered signal intensity in the affected or contralateral hippocampus in individuals with MRI-negative mTLE, both in the evaluation of the entire hippocampus and in a separate analysis of the presubiculum.

3.3 | Comparison between histological HS subtypes

A volumetric comparison of the HS1 and HS2 subtypes within the HS-mTLE sample did not reveal any significant subfield-specific differences, see Online Table 7.

A point-wise comparison of hippocampal thickness values between HS1 and HS2 also revealed no significant differences. In a next step, curvature values were assessed along the medial-lateral axis. It is noticeable that the average of all three subjects with HS3 shows a peak in curvature in the CA1 region, which can also be seen in the individual graphs of HS3 individuals (Figure 4). This peak cannot

be found in the average graphs of HS1 and HS2. Due to a small sample size of the HS3 group, we refrained from statistical testing at this point.

3.4 | Impaired versus non-impaired verbal memory

A point-wise analysis of hippocampal thickness unveiled no significant differences of the affected or of the contralateral hippocampus in subjects with impaired verbal memory compared to individuals with unimpaired verbal memory.

Additionally, as verbal memory is known to be lateralized, we used a native left/right orientation, no longer distinguishing between affected and contralateral sides. In the right hippocampus, this yielded no significant differences between subjects with impaired and unimpaired verbal memory.

In the left hippocampus, however, we observed a cluster with significantly lower hippocampal thickness (FWER-corrected $p < .05$) in the presubiculum and medial part of the subiculum (Figure 5).

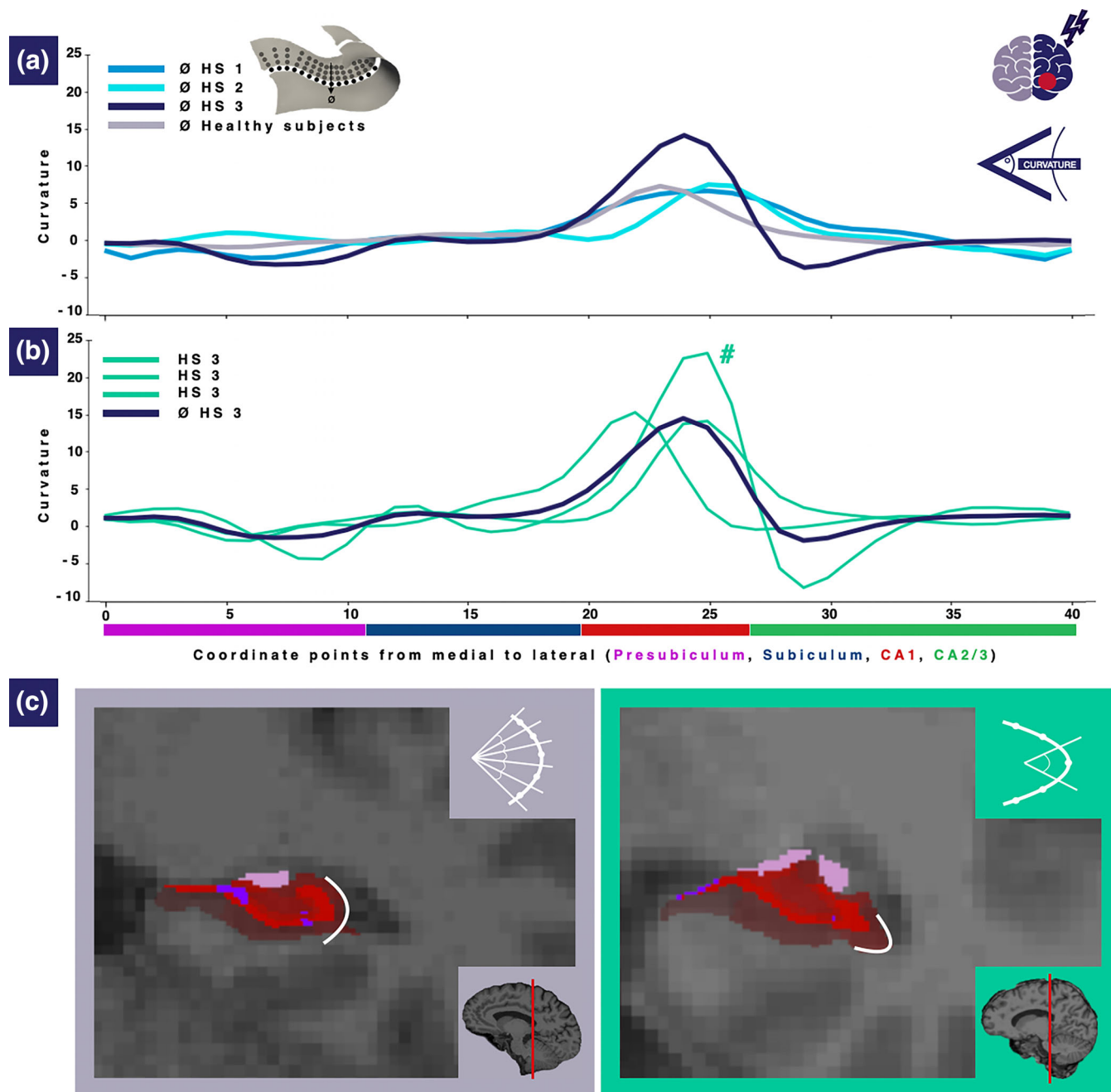


FIGURE 4 Mapping of curvature values along the medial-lateral axis of the affected hippocampus of HS-mTLE subtypes (HS1, HS2, and HS3). (a) Mapping of the average curvature values of HS1, HS2, and HS3 subgroups and healthy subjects along the medial-lateral axis of the affected hippocampus. (b) Mapping of curvature values of the individuals in the HS3 subgroup and average curvature values of the HS3 subgroup along the medial-lateral axis of the affected hippocampus. #: marks the individual with HS3 whose affected hippocampus is presented in (c). (c) Left: FreeSurfer output of the left hippocampus of a healthy subject. Right: FreeSurfer output of the affected, left hippocampus of a HS3 individual. Top inlay demonstrates the angles calculated in the curvature feature. Below inlay shows the coronal plane of which the photo was taken. CA, cornu ammonis; HS-mTLE, hippocampal sclerosis in individuals with mesial temporal lobe epilepsy.

4 | DISCUSSION

In this retrospective study, we examined the internal structure of the hippocampus using a novel geometry-based algorithm in a cohort of 204 individuals with HS-mTLE or MRI-negative mTLE and compared our results to conventional volumetric measurements.

4.1 | Point-wise analysis uncovers structural alterations missed by conventional volumetry

In the affected hippocampus of individuals with HS-mTLE, the novel point-wise analysis revealed areas with lower hippocampal thickness and higher FLAIR signal intensities as compared to

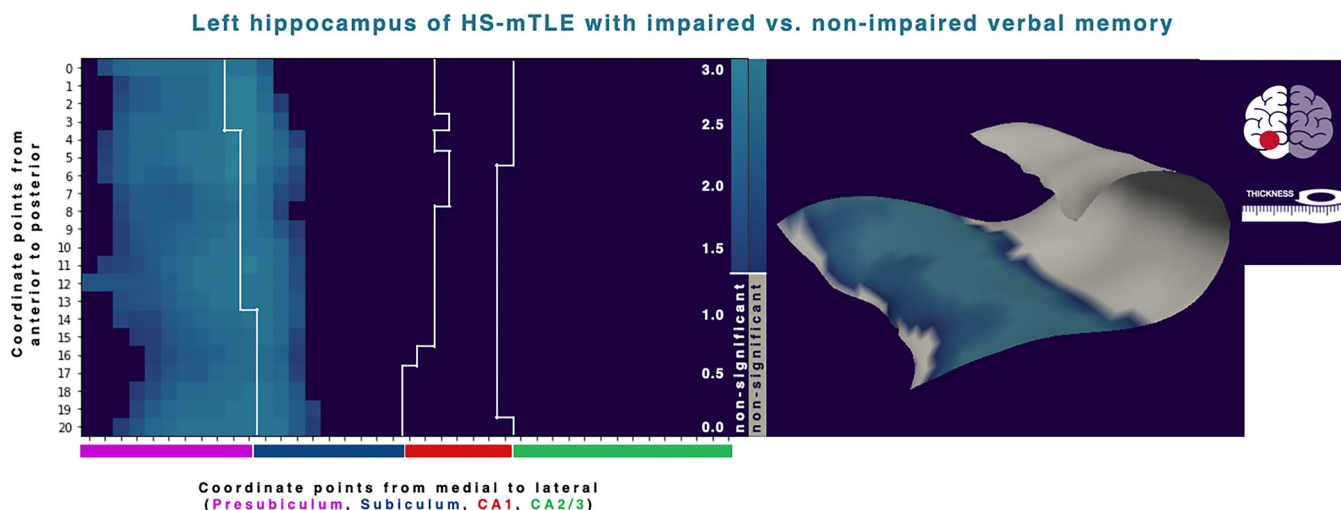


FIGURE 5 Left hippocampus of HS-mTLE with impaired versus non-impaired verbal memory: Thickness analysis. Left: Negative logarithms of significant p -values mapped along the intrinsic coordinate system of the hippocampus. Non-significant points are shown in dark-blue color. White lines: plotted boundaries of subfields, colored bars correspond to subfields. Right: Mapping of the negative logarithms of significant p -values onto the medial surface of a control hippocampus. CA, cornu ammonis; HS-mTLE, hippocampal sclerosis in individuals with mesial temporal lobe epilepsy.

healthy subjects throughout the entire hippocampus, which meets expectations and is confirmed by the results of conventional volumetric measurements showing lower volumes of almost all hippocampal subfields. It should not be dismissed that the FLAIR signal, albeit normalized may be ill-defined and only carefully used as a quantitative metric. Particularly, there is no canonic approach to the intensity normalization of the FLAIR-signal. The method used here has been tested in previous studies (Focke et al., 2008, 2009; Huppertz et al., 2011; Wagner et al., 2013) and we compared it to a simple normalization, which yielded the same results.

In the contralateral hemisphere, we observed no volumetric alterations in the subfields covered by the point-wise approach. In point-wise analysis, however, lower hippocampal thickness as compared to controls was observed in the entire presubiculum, without any corresponding significant FLAIR signal alteration. Most interestingly, point-wise analysis showed lower hippocampal thickness in the presubiculum of the affected hippocampus in individuals with MRI-negative mTLE as compared to healthy subjects, while conventional volumetric analyses revealed no significant differences. Hence, the novel geometry-based approach applied in this study can uncover structural alterations of the hippocampus not measurable by conventional volumetry.

It is worth noting that different MRI scanners were used for the images of the HS-mTLE group, which may bias the segmentation of hippocampal subfields in FreeSurfer (Brown et al., 2020; Quattrini et al., 2020). This effect is controlled for by the covariate sequence in our statistical analysis. However, this effect is only estimated in the HS-mTLE group, although ideally it would be estimated across all groups.

4.2 | Geometry-based point-wise analysis extends the scope of hippocampal morphometry

Another advantage of the proposed geometry-based approach lies in its ability to assess a set of geometrical properties of the hippocampus beyond thickness. This includes curvature, which can be understood as a proxy measure for the volume of the medial CA4 subfield and the dentate gyrus. For instance, lower volumes of the dentate gyrus, a structure that lies within the “C”-shaped CA, would theoretically result in a compression of the “C”-shape and therefore in a higher curvature mostly in the CA1 region (see Figure 4). In our study, this feature was proven successful in differentiating between the HS1/HS2 and HS3 subtype, which is histologically defined by cell loss mostly in the CA4 subfield (Blümcke et al., 2013; see Table 1). These differences could even be seen on a single case level.

However, both the point-wise analysis and the volumetry performed in this study rely on FreeSurfer-derived segmentations of hippocampal subfields and are therefore closely related. Regarding subfield delineation, the boundaries projected onto the internal coordinate system are mappings from the image-based segmentation to the hippocampal midplane. Therefore, the same limitations as for the boundaries in the original segmentation apply. Nevertheless, the geometry-based method improves this specific aspect in two ways: First, for the construction of the internal coordinate system and the estimation of hippocampal thickness and curvature, only the segmentation of the hippocampal body, but no subfield boundaries are required. Second, point-wise analysis permits the detection of effects that cover only part of a given subfield or extend across the borders of subfields, therefore reducing the need to rely on subfield boundaries.

Taken together, our results reach in multiple aspects beyond the scope of conventional volumetric measures. This raises hope that a point-wise geometry-based approach may on a long-run improve imaging-based preoperative evaluation of mTLE and diminish the group of MRI-negative cases in clinical practice.

4.3 | Geometry-based hippocampal morphometry is linked to clinical markers

Looking at the clinical picture of mTLE, verbal memory impairment ranks among the most relevant clinical markers for disease severity (Helmstaedter & Kockelmann, 2006). Previous research has outlined in manifold ways that verbal memory performance is linked to structural integrity of the left hippocampus (Postma et al., 2020; Sidhu et al., 2013; Weintrob et al., 2002; Witt et al., 2014). However, literature is ambiguous on whether there is an association of verbal memory performance with alterations in a specific hippocampal subfield or rather with the integrity of the entire hippocampus (Comper et al., 2017; Coras et al., 2014; Ono et al., 2021; Sass et al., 1992; Witt et al., 2015). Our point-wise analysis adds to this by showing lower hippocampal thickness in individuals with HS-mTLE and impaired verbal memory than in persons with HS-mTLE and unimpaired verbal memory specifically in the presubiculum and subiculum of the left hippocampus. In the right hippocampus, we did not observe any differences.

4.4 | Pathomechanic implications of point-wise morphometry in TLE

Regarding the pathomechanisms underlying mTLE, our novel morphometric results yield two common aspects: First, despite the more fine-grained spatial resolution as compared to subfield-level volumetric measures, all structural alterations we observed follow the internal subfield architecture and an anterior-posterior axis of the hippocampus, which has recently been shown to form the main organizational gradient regarding anatomical and functional properties (Strange et al., 2014; Vos de Wael et al., 2018). Second, lower thickness of the presubiculum is commonly found in hippocampi that were supposedly nonlesional, such as in MRI-negative individuals and in the contralateral side in individuals with HS-mTLE. Previous research has hypothesized that structural alterations of the presubiculum in mTLE may rather be due to epileptic seizures than to the primary pathological process (Maccotta et al., 2015). Considering that in our study structural alterations in the presubiculum were not accompanied by higher FLAIR signal intensity, and even signal alterations in the affected hippocampus in HS-mTLE excluded the presubiculum, it appears indeed unlikely that this subfield is involved in the primary inflammatory process. In this respect, our results support the hypothesis of potentially bilateral secondary degeneration of the presubiculum as proposed by Maccotta and colleagues. Furthermore, the geometry-based method finds structural changes in the

presubiculum on the affected side of MRI-negative mTLE without detectable signs of active inflammation. This result may be predicted in that we cannot exclude the possibility that there are cases of HS in this group because histopathologic workup was not available in the 49/58 MRI-negative subjects who did not undergo surgery. Previous studies have shown that interictal connectivity also differs between MRI-negative mTLE and HS-mTLE with a lack of involvement of mesiotemporal regions in MRI-negative mTLE (Vaughan et al., 2016). Our findings support the hypothesis that mesiotemporal structures are not primarily involved in epileptogenesis in MRI-negative mTLE and that HS-mTLE and MRI-negative mTLE are different pathologies.

4.5 | Limitations

The aspects that limit the explanatory power of our data are three-fold: A first limitation of our study lies in its cross-sectional design, which is challenged by therapeutic interventions. As mTLE is one of the major causes for medically refractory epilepsy, it must be assumed that all individuals with mTLE seeking care at a tertiary epilepsy center have been exposed to different and highly individual therapy regimes regarding antiepileptic drugs, which themselves are known to have an effect on both cognition and structural integrity of brain structures and are not incorporated in the statistical models (Brunbech & Sabers, 2002; Quon et al., 2020). A second limitation concerns statistical aspects, such as the fact that our HS3 cohort consists of too few subjects to perform meaningful statistical analyses. In addition, all analyses presented in this study were performed at the group level. To adopt the novel approach in a clinical setting, however, it would also need to be applicable at subject-level, which ideally needs to be demonstrated in a prospective design. Third, the histologic underpinnings of the proposed geometry-derived measurements remain speculative. Although it seems logical that the reduced thickness and increased curvature are due to cell loss in specific subunits of the hippocampus, this direct correlation would need to be demonstrated by ex-vivo histological studies.

5 | CONCLUSION

In conclusion, our study established and applied a novel geometry-based analysis approach to hippocampal structure and has proven it to be useful in individuals with mTLE. We demonstrated that this approach, with its extended imaging markers, has surplus value over conventional volumetric analysis of the hippocampus with respect to diagnostic and pathophysiological implications, raising hope that this or similar methods will find their way into clinical practice.

ACKNOWLEDGMENTS

This work was not supported by specific funding. Tobias Bauer and Laura Fischbach were supported by the BONFOR research commission of the medical faculty of the University of Bonn (grant numbers:

2019-4-07, 2020-4-06). Open Access funding enabled and organized by Projekt DEAL.

CONFLICT OF INTEREST STATEMENT

Laura Fischbach, Tobias Bauer, Kersten Diers, Mar Bragues, Martin Schidlowski, Attila Rácz, Tobias Baumgartner, Hartmut Vatter, Albert J. Becker, Daniel Paech, Bernd Weber, and Martin Reuter declare no conflicts of interest. Juri-Alexander Witt reports personal fees from Eisai. These activities were not related to the content of this manuscript. Valeri Borger has received fees for serving as clinical consultant from Brainlab AG. These activities were not related to the content of this manuscript. Randi von Wrede has received travel support, fees as speaker or for serving on the advisory board from Angelini, Apocare, Arvelle, Cerbomed, Desitin, Eisai, GW pharmaceuticals-JAZZ pharma and UCB Pharma. These activities were not related to the content of this manuscript. Alexander Radbruch serves on the scientific advisory boards for GE Healthcare, Bracco, Bayer, Guerbet, and AbbVie; has received speaker honoraria from Bayer, Guerbet, Siemens, and Medscape; and is a consultant for, and has received institutional study support from, Guerbet and Bayer. Hans-Jürgen Huppertz is the author of MAP18. The program is available for other epilepsy centers on request. In this case, the Swiss Epilepsy Clinic, Dr. Huppertz's employer, charges a fee for creating a scanner-specific normal database. Christoph Helmstaedter has received grants from the European Union, travel support from Desitin, honoraria for lectures, counseling, and advisory boards from GW Pharmaceuticals, Eisai, and UCB, as well as license fees from Eisai and UCB. Rainer Surges has received fees as speaker or for serving on the advisory board from Angelini, Arvelle, Bial, Desitin, Eisai, Janssen-Cilag GmbH, LivaNova, Novartis, Precisis GmbH, UCB Pharma, UnEEG and Zogenix and grants from the Deutsche Forschungsgemeinschaft (DFG), the Bundesministerium für Bildung und Forschung (BMBF), the Bundesministerium für Gesundheit, and the Marga and Walter Boll Stiftung. These activities were not related to the content of this manuscript. Theodor Rüber declares that the research was conducted in the absence of any commercial or financial relationships that could be construed as a potential conflict of interest. The results were presented in a poster at the DGFE 2022 in Leipzig/Germany and at the OHBM 2022 in Glasgow/UK.

DATA AVAILABILITY STATEMENT

The data that support the findings of this study are available on request from the corresponding author. The data are not publicly available due to privacy or ethical restrictions.

ORCID

Tobias Bauer  <https://orcid.org/0000-0002-0555-6214>

Theodor Rüber  <https://orcid.org/0000-0002-6180-7671>

REFERENCES

- Blümcke, I., Beck, H., Lie, A. A., & Wiestler, O. D. (1999). Molecular neuropathology of human mesial temporal lobe epilepsy. *Epilepsy Research*, 36(2–3), 205–223. [https://doi.org/10.1016/s0920-1211\(99\)00052-2](https://doi.org/10.1016/s0920-1211(99)00052-2)
- Blümcke, I., Coras, R., Miyata, H., & Ozkara, C. (2012). Defining clinico-neuropathological subtypes of mesial temporal lobe epilepsy with hippocampal sclerosis. *Brain Pathology*, 22(3), 402–411. <https://doi.org/10.1111/j.1750-3639.2012.00583.x>
- Blümcke, I., Pauli, E., Clusmann, H., Schramm, J., Becker, A., Elger, C., Merschhemke, M., Meencke, H. J., Lehmann, T., Von Deimling, A., Scheiwe, C., Zentner, J., Volk, B., Romstöck, J., Stefan, H., & Hildebrandt, M. (2007). A new clinico-pathological classification system for mesial temporal sclerosis. *Acta Neuropathologica*, 113(3), 235–244. <https://doi.org/10.1007/s00401-006-0187-0>
- Blümcke, I., Thom, M., Aronica, E., Armstrong, D. D., Bartolomei, F., Bernasconi, A., Bernasconi, N., Bien, C. G., Cendes, F., Coras, R., Cross, J. H., Jacques, T. S., Kahane, P., Mathern, G. W., Miyata, H., Moshé, S. L., Oz, B., Özkara, Ç., Perucca, E., ... Spreafico, R. (2013). International consensus classification of hippocampal sclerosis in temporal lobe epilepsy: A task force report from the ILAE commission on diagnostic methods. *Epilepsia*, 54(7), 1315–1329. <https://doi.org/10.1111/epi.12220>
- Blümcke, I., Thom, M., & Wiestler, O. D. (2002). Ammon's horn sclerosis: A maldevelopmental disorder associated with temporal lobe epilepsy. *Brain Pathology*, 12(2), 199–211. <https://doi.org/10.1111/j.1750-3639.2002.tb00436.x>
- Brown, E. M., Pierce, M. E., Clark, D. C., Fischl, B. R., Iglesias, J. E., Milberg, W. P., McGlinchey, R. E., & Salat, D. H. (2020). Test-retest reliability of FreeSurfer automated hippocampal subfield segmentation within and across scanners. *NeuroImage*, 210, 116563. <https://doi.org/10.1016/j.neuroimage.2020.116563>
- Brunbech, L., & Sabers, A. (2002). Effect of antiepileptic drugs on cognitive function in individuals with epilepsy: A comparative review of newer versus older agents. *Drugs*, 62(4), 593–604. <https://doi.org/10.2165/00003495-200262040-00004>
- Comper, S. M., Jardim, A. P., Corso, J. T., Gaça, L. B., Noffs, M. H. S., Lancellotti, C. L. P., Cavalheiro, E. A., Centeno, R. S., & Yacubian, E. M. T. (2017). Impact of hippocampal subfield histopathology in episodic memory impairment in mesial temporal lobe epilepsy and hippocampal sclerosis. *Epilepsy & Behavior*, 75, 183–189. <https://doi.org/10.1016/j.yebeh.2017.08.013>
- Coras, R., & Blümcke, I. (2015). Clinico-pathological subtypes of hippocampal sclerosis in temporal lobe epilepsy and their differential impact on memory impairment. *Neuroscience*, 309, 153–161. <https://doi.org/10.1016/j.neuroscience.2015.08.003>
- Coras, R., Pauli, E., Li, J., Schwarz, M., Rössler, K., Buchfelder, M., Hamer, H., Stefan, H., & Blümcke, I. (2014). Differential influence of hippocampal subfields to memory formation: Insights from patients with temporal lobe epilepsy. *Brain*, 137(7), 1945–1957. <https://doi.org/10.1093/brain/awu100>
- Dale, A. M., Fischl, B., & Sereno, M. I. (1999). Cortical surface-based analysis. I. Segmentation and surface reconstruction. *NeuroImage*, 9, 179–194.
- Diers, K., Baumeister, H., Jessen, F., Düzel, E., Berron, D., & Reuter, M. (2023). An automated, geometry-based method for the analysis of hippocampal thickness. *NeuroImage*, 276, 120182. <https://doi.org/10.1016/j.neuroimage.2023.120182>
- Engel, J., Jr. (1996). Introduction to temporal lobe epilepsy. *Epilepsy Research*, 26(1), 141–150. [https://doi.org/10.1016/s0920-1211\(96\)00043-5](https://doi.org/10.1016/s0920-1211(96)00043-5)
- Focke, N. K., Bonelli, S. B., Yogarajah, M., Scott, C., Symms, M. R., & Duncan, J. S. (2009). Automated normalized FLAIR imaging in MRI-negative patients with refractory focal epilepsy. *Epilepsia*, 50(6), 1484–1490. <https://doi.org/10.1111/j.1528-1167.2009.02022.x>
- Focke, N. K., Symms, M. R., Burdett, J. L., & Duncan, J. S. (2008). Voxel-based analysis of whole brain FLAIR at 3T detects focal cortical dysplasia. *Epilepsia*, 49(5), 786–793. <https://doi.org/10.1111/j.1528-1167.2007.01474.x>

- Gramfort, A., Luessi, M., Larson, E., Engemann, D. A., Strohmeier, D., Brodbeck, C., Parkkonen, L., & Hämäläinen, M. S. (2014). MNE software for processing MEG and EEG data. *NeuroImage*, 86, 446–460. <https://doi.org/10.1016/j.neuroimage.2013.10.027>
- Helmstaedter, C., & Durwen, H. F. (1990). VLMT: Verbaler Lern- und Merkfähigkeitstest: Ein praktikables und differenziertes Instrumentarium zur Prüfung der verbalen Gedächtnisleistungen. *Schweizer Archiv für Neurologie, Neurochirurgie Und Psychiatrie*, 141, 21–30.
- Helmstaedter, C., & Kockelmann, E. (2006). Cognitive outcomes in patients with chronic temporal lobe epilepsy. *Epilepsia*, 47(2), 96–98. <https://doi.org/10.1111/j.1528-1167.2006.00702.x>
- Helmstaedter, C., Pohl, C., Hufnagel, A., & Elger, C. E. (1991). Visual learning deficits in nonresected patients with right temporal lobe epilepsy. *Cortex*, 27, 547–555.
- Huppertz, H.-J., Wagner, J., Weber, B., House, P., & Urbach, H. (2011). Automated quantitative FLAIR analysis in hippocampal sclerosis. *Epilepsy Research*, 97(1–2), 146–156. <https://doi.org/10.1016/j.eplepsyres.2011.08.001>
- Iglesias, J. E., Augustinack, J. C., Nguyen, K., Player, C. M., Player, A., Wright, M., Roy, N., Frosch, M. P., McKee, A., Wald, L. L., Fischl, B., Van Leemput, K., & Alzheimer's Disease Neuroimaging Initiative. (2015). A computational atlas of the hippocampal formation using ex vivo, ultra-high resolution MRI: Application to adaptive segmentation of in vivo MRI. *NeuroImage*, 115, 117–137. <https://doi.org/10.1016/j.neuroimage.2015.04.042>
- Immonen, A., Jutila, L., Muraja-Murro, A., Mervaala, E., Äikiä, M., Lamusuo, S., Kuikka, J., Vanninen, E., Alafuzoff, I., Ikonen, A., Vanninen, R., Vapalahti, M., & Kälviäinen, R. (2010). Long-term epilepsy surgery outcomes in patients with MRI-negative temporal lobe epilepsy. *Epilepsia*, 51(11), 2260–2269. <https://doi.org/10.1111/j.1528-1167.2010.02720.x>
- Jolly, E. (2018). Pymer4: Connecting R and python for linear mixed modeling. *Journal of Open Source Software*, 3(31), 862. <https://doi.org/10.21105/joss.00862>
- Maccotta, L., Moseley, E. D., Benzinger, T. L., & Hogan, R. E. (2015). Beyond the CA1 subfield: Local hippocampal shape changes in MRI-negative temporal lobe epilepsy. *Epilepsia*, 56(5), 780–788. <https://doi.org/10.1111/epi.12955>
- Muhlhofer, W., Tan, Y. L., Mueller, S. G., & Knowlton, R. (2017). MRI-negative temporal lobe epilepsy-what do we know? *Epilepsia*, 58(5), 727–742. <https://doi.org/10.1111/epi.13699>
- Ono, S. E., Mader-Joaquim, M. J., de Carvalho, N. A., de Paola, L., Dos Santos, G. R., & Silvado, C. E. S. (2021). Relationship between hippocampal subfields and verbal and visual memory function in mesial temporal lobe epilepsy patients. *Epilepsy Research*, 175, 106700. <https://doi.org/10.1016/j.eplepsyres.2021.106700>
- Opheim, G., van der Kolk, A., Markenroth Bloch, K., et al. (2021). 7T epilepsy task force consensus recommendations on the use of 7T MRI in clinical practice. *Neurology*, 96(7), 327–341. <https://doi.org/10.1212/WNL.00000000000011413>
- Postma, T. S., Cury, C., Baxendale, S., Thompson, P. J., Cano-López, I., Tisi, J., Burdett, J. L., Sidhu, M. K., Caciagli, L., Winston, G. P., Vos, S. B., Thom, M., Duncan, J. S., Koepp, M. J., & Galovic, M. (2020). Hippocampal shape is associated with memory deficits in temporal lobe epilepsy. *Annals of Neurology*, 88(1), 170–182. <https://doi.org/10.1002/ana.25762>
- Quattrini, G., Pievani, M., Jovicich, J., Aiello, M., Bargalló, N., Barkhof, F., Bartres-Faz, D., Beltramello, A., Pizzini, F. B., Blin, O., Bordet, R., Caulo, M., Constantinides, M., Didic, M., Drevelegas, A., Ferretti, A., Fiedler, U., Floridi, P., Gros-Dagnac, H., ... PharmaCog Consortium. (2020). Amygdalar nuclei and hippocampal subfields on MRI: Test-retest reliability of automated volumetry across different MRI sites and vendors. *NeuroImage*, 218, 116932. <https://doi.org/10.1016/j.neuroimage.2020.116932>
- Quon, R. J., Mazanec, M. T., Schmidt, S. S., Andrew, A. S., Roth, R. M., MacKenzie, T. A., Sajatovic, M., Spruill, T., & Jobst, B. C. (2020). Antiepileptic drug effects on subjective and objective cognition. *Epilepsy & Behavior*, 104, 106906. <https://doi.org/10.1016/j.yebeh.2020.106906>
- Saghafi, S., Ferguson, L., Hogue, O., Gales, J. M., Prayson, R., & Busch, R. M. (2018). Histopathologic subtype of hippocampal sclerosis and episodic memory performance before and after temporal lobectomy for epilepsy. *Epilepsia*, 59(4), 825–833. <https://doi.org/10.1111/epi.14036>
- Santyr, B. G., Goubran, M., Lau, J. C., Kwan, B. Y. M., Salehi, F., Lee, D. H., Mirsattari, S. M., Burneo, J. G., Steven, D. A., Parrent, A. G., Ribaupierre, S., Hammond, R. R., Peters, T. M., & Khan, A. R. (2017). Investigation of hippocampal substructures in focal temporal lobe epilepsy with and without hippocampal sclerosis at 7T. *Journal of Magnetic Resonance Imaging*, 45(5), 1359–1370. <https://doi.org/10.1002/jmri.25447>
- Sass, K. J., Sass, A., Westerveld, M., Lencz, T., Novelly, R. A., Kim, J. H., & Spencer, D. D. (1992). Specificity in the correlation of verbal memory and hippocampal neuron loss: Dissociation of memory, language, and verbal intellectual ability. *Journal of Clinical and Experimental Neuropsychology*, 14(5), 662–672. <https://doi.org/10.1080/01688639208402854>
- Saygin, Z. M., Kliemann, D., Iglesias, J. E., van der Kouwe, A., Boyd, E., Reuter, M., Stevens, A., van Leemput, K., McKee, A., Frosch, M. P., Fischl, B., Augustinack, J. C., & Alzheimer's Disease Neuroimaging Initiative. (2017). High-resolution magnetic resonance imaging reveals nuclei of the human amygdala: Manual segmentation to automatic atlas. *NeuroImage*, 155, 370–382. <https://doi.org/10.1016/j.neuroimage.2017.04.046>
- Schwartzkroin, P. A. (1986). Hippocampal slices in experimental and human epilepsy. *Advances in Neurology*, 44, 991–1010.
- Seabold, S., & Perktold, J. (2010). Statsmodels: Econometric and statistical modeling with Python. *Proceedings of the 9th Python in Science Conference* 2010, 92–96.
- Semah, F., Picot, M. C., Adam, C., Broglin, D., Arzimanoglou, A., Bazin, B., Cavalcanti, D., & Baulac, M. (1998). Is the underlying cause of epilepsy a major prognostic factor for recurrence? *Neurology*, 51(5), 1256–1262. <https://doi.org/10.1212/wnl.51.5.1256>
- Sidhu, M. K., Stretton, J., Winston, G. P., Bonelli, S., Centeno, M., Vollmar, C., Symms, M., Thompson, P. J., Koepp, M. J., & Duncan, J. S. (2013). A functional magnetic resonance imaging study mapping the episodic memory encoding network in temporal lobe epilepsy. *Brain*, 136(6), 1868–1888. <https://doi.org/10.1093/brain/awt099>
- Stefan, H., Hildebrandt, M., Kerling, F., Kasper, B. S., Hammen, T., Dorfler, A., Weigel, D., Buchfelder, M., Blumcke, I., & Pauli, E. (2009). Clinical prediction of postoperative seizure control: Structural, functional findings and disease histories. *Journal of Neurology, Neurosurgery, and Psychiatry*, 80(2), 196–200. <https://doi.org/10.1136/jnnp.2008.151860>
- Strange, B. A., Witter, M. P., Lein, E. S., & Moser, E. I. (2014). Functional organization of the hippocampal longitudinal axis. *Nature Reviews. Neuroscience*, 15(10), 655–669. <https://doi.org/10.1038/nrn3785>
- Téllez-Zenteno, J. F., & Hernández-Ronquillo, L. (2012). A review of the epidemiology of temporal lobe epilepsy. *Epilepsy Research and Treatment*, 2012, 630853. <https://doi.org/10.1155/2012/630853>
- Thom, M. (2014). Review: Hippocampal sclerosis in epilepsy: A neuropathology review. *Neuropathology and Applied Neurobiology*, 40(5), 520–543. <https://doi.org/10.1111/nan.12150>
- Vaughan, D. N., Rayner, G., Tailby, C., & Jackson, G. D. (2016). MRI-negative temporal lobe epilepsy: A network disorder of neocortical connectivity. *Neurology*, 87(18), 1934–1942. <https://doi.org/10.1212/WNL.0000000000003289>
- Virtanen, P., Gommers, R., Oliphant, T. E., Haberland, M., Reddy, T., Cournapeau, D., Burovski, E., Peterson, P., Weckesser, W., Bright, J., van der Walt, S. J., Brett, M., Wilson, J., Millman, K. J., Mayorov, N., Nelson, A. R. J., Jones, E., Kern, R., Larson, E., ... Vázquez-Baeza, Y.

- (2020). SciPy 1.0: Fundamental algorithms for scientific computing in Python. *Nature Methods*, 17(3), 261–272. <https://doi.org/10.1038/s41592-019-0686-2>
- Vos de Wael, R., Larivière, S., Caldaïrou, B., Hong, S. J., Margulies, D. S., Jefferies, E., Bernasconi, A., Smallwood, J., Bernasconi, N., & Bernhardt, B. C. (2018). Anatomical and microstructural determinants of hippocampal subfield functional connectome embedding. *Proceedings of the National Academy of Sciences of the United States of America*, 115(40), 10154–10159. <https://doi.org/10.1073/pnas.1803667115>
- Wachinger, C., Salat, D. H., Weiner, M., & Reuter, M. (2016). Alzheimer's disease neuroimaging initiative. Whole-brain analysis reveals increased neuroanatomical asymmetries in dementia for hippocampus and amygdala. *Brain*, 139(12), 3253–3266. <https://doi.org/10.1093/brain/aww243>
- Wagner, J., Schoene-Bake, J.-C., Malter, M. P., Urbach, H., Huppertz, H.-J., Elger, C. E., & Weber, B. (2013). Quantitative FLAIR analysis indicates predominant affection of the amygdala in antibody-associated limbic encephalitis. *Epilepsia*, 54(9), 1679–1687. <https://doi.org/10.1111/epi.12320>
- Wang, I., Oh, S., Blümcke, I., Coras, R., Krishnan, B., Kim, S., McBride, A., Grinenko, O., Lin, Y., Overmyer, M., Aung, T. T., Lowe, M., Larvie, M., Alexopoulos, A. V., Bingaman, W., Gonzalez-Martinez, J. A., Najm, I., & Jones, S. E. (2020). Value of 7T MRI and post-processing in patients with nonlesional 3T MRI undergoing epilepsy presurgical evaluation. *Epilepsia*, 61(11), 2509–2520. <https://doi.org/10.1111/epi.16682>
- Weintrob, D. L., Saling, M. M., Berkovic, S. F., Berlangieri, S. U., & Reutens, D. C. (2002). Verbal memory in left temporal lobe epilepsy: Evidence for task-related localization. *Annals of Neurology*, 51(4), 442–447. <https://doi.org/10.1002/ana.10133>
- Wieser, H. G. (1988). Selective amygdalo-hippocampectomy for temporal lobe epilepsy. *Epilepsia*, 29(2), S100–S113. <https://doi.org/10.1111/j.1528-1157.1988.tb05793.x>
- Witt, J. A., Coras, R., Schramm, J., Becker, A. J., Elger, C. E., Blümcke, I., & Helmstaedter, C. (2014). The overall pathological status of the left hippocampus determines preoperative verbal memory performance in left mesial temporal lobe epilepsy. *Hippocampus*, 24(4), 446–454. <https://doi.org/10.1002/hipo.22238>
- Witt, J. A., Helmstaedter, C., & Elger, C. E. (2015). Is there evidence of a subordinate role of the hippocampal CA1 field for declarative memory formation? *Brain*, 138(4), e343. <https://doi.org/10.1093/brain/awu303>
- Yin, Z. R., Kang, H. C., Wu, W., Wang, M., & Zhu, S. Q. (2013). Do neuroimaging results impact prognosis of epilepsy surgery? A meta-analysis. *Journal of Huazhong University of Science and Technology. Medical Sciences*, 33(2), 159–165. <https://doi.org/10.1007/s11596-013-1090-2>

SUPPORTING INFORMATION

Additional supporting information can be found online in the Supporting Information section at the end of this article.

How to cite this article: Fischbach, L., Bauer, T., Diers, K., Witt, J.-A., Bragues, M., Borger, V., Schidlowski, M., Rácz, A., Baumgartner, T., von Wrede, R., Paech, D., Weber, B., Radbruch, A., Vatter, H., Becker, A. J., Huppertz, H.-J., Helmstaedter, C., Surges, R., Reuter, M., & Rüber, T. (2023). A novel geometry-based analysis of hippocampal morphometry in mesial temporal lobe epilepsy. *Human Brain Mapping*, 44(12), 4467–4479. <https://doi.org/10.1002/hbm.26392>